MULTIPLE-INLET BIPV/T: MODELLING AND DESIGN INCLUDING WIND EFFECTS

Efstratios Dimitrios Rounis[1], Andreas Athienitis[1], Theodore Stathopoulos[1]
[1]Department of Building, Civil and Environmental Engineering, Concordia University, Montreal, Quebec, Canada

ABSTRACT

Multiple-inlet Building-integrated Photovoltaic/ Thermal (BIPV/T) systems aim for an improved electrical and thermal performance, as well as durability, by enhancing the heat removal from the PV panels, while achieving lower and more uniform PV temperatures.

This paper presents the results of a numerical investigation on the comparison of the performance of single and multiple-inlet BIPV/T systems for a large scale application on an office building, under varying weather conditions, in terms of electrical and thermal efficiency of the systems, as well as the PV temperature distributions. A complete modeling procedure for multiple-inlet BIPV/T is introduced for the first time.

It was found that a properly designed multiple-inlet BIPV/T system may have higher electrical efficiency up to 1% (approximately 7% higher electrical production for a 120 kW system) and higher thermal efficiency and up to 24%, while resulting in the lowest and most uniform PV temperatures.

INTRODUCTION

Integration of PV modules with the building envelope has proven to be a highly efficient way of employing solar technology. PV becomes thus part of a holistic design of a building or a retrofit, increasing its cost-effectiveness by replacing common building materials (Athienitis et al, 2010).

BIPV/T systems combine the features of a solar collector and a PV system, while the PV layer may act as a rain-screen cladding. A channel is formed between the PV layer and the internal skin of the building, within which a fluid medium circulates, extracting heat from the PV via convection. Apart from the potential thermal gains, heat extraction from the PV results to enhanced system durability, as well as enhanced electrical production, since, according to Florschuetz (1979), the electrical efficiency of the PV module is a function of its temperature. It becomes clear that low operating temperatures can be crucial for the performance of the systems, especially in large installations. Depending on the cooling fluid medium used, BIPV/T systems are divided into air-based and water-based systems. Water-based systems have higher heat exchange efficiency, due to the higher specific heat capacity and density of water. However, air-based systems are more practical for large applications since they pose no leakage issues through ducts and joints, there is no need for the addition of anti-freezing additives, they are lighter, easier to install and maintain and far less complicated.

In order to compensate for the low heat exchange efficiency of air-based systems, several studies have been carried out in to investigate heat transfer enhancement techniques. These techniques include the addition of a top glazing part to reduce wind induced thermal losses (Hegazy, 1999) and double pass configurations, to the use of thin metal plates and fins to enhance internal convection (Tonui & Tripanagnostopoulos, 2006). Most of these techniques achieve higher air temperature at the air-collector outlet, also resulting in higher PV temperatures. Higher air collection rate has in all cases resulted in lower PV temperatures. However, that was at the cost of additional fan power consumption, which reduced the net electrical gain, while the continuous air channel of the considered configurations resulted in a PV temperature stratification, the warmest PV modules located near the air collector outlet. This could lead to non-uniform electrical performance of the system, quicker degradation of the panels operating at higher temperatures, as well as differential expansion issues that could harm the bearing mechanism, as was discussed by Yang, 2014.

MULTIPLE-INLET BIPV/T

A potential method that could counter the effect of temperature stratification and yield lower PV temperatures is the employment of more than one opening on the PV system along the flow path of the air channel, as shown in Figure 1.

This technique results in separate channels, one for each PV module. These channels are interconnected and form a multiple-inlet system with a central air collector. The aim of such systems is the enhancement of heat extraction by regulating both the flow of each channel, as well as the thermal boundary conditions of air entering each channel opening.

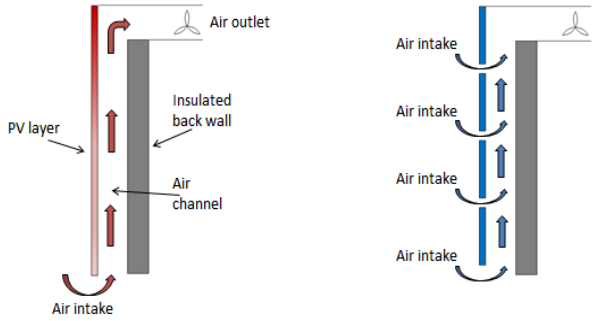

Figure 1: Single and multiple-inlet BIPV/T system.

The literature on such systems is limited, as these are a rather new concept. An early form of a multiple-inlet BIPV/T was introduced by Athenitis et al, 2010. The developed prototype of the study, also applied on the JMSB building of Concordia University, consisted of a layer of unglazed transpired collector (UTC), upon which PV modules were fixed with supports. The PV covered 70% of the system's area, while air entered the system from openings below the PV modules and through the UTC perforation. The concept of the system was that the solar collector could also produce electrical energy, increasing its cost-effectiveness, especially in the summer months, during which space heating is not needed (except for domestic water heating use). The overall thermal performance of the hybrid system was lower than that of a UTC. However, if the electrical energy produced was expressed in terms of equivalent thermal energy, the overall efficiency of the hybrid system was found to be 7-17% higher than that of the UTC (Athienitis et al, 2010; Bambara et al, 2012). The term "equivalent thermal energy" was developed for that specific study in order to compare different systems, with the assumption that one unit of electrical energy equals to four units of thermal energy, if the average coefficient of performance (COP) of a heat pump (4) is taken into account. The system was modelled assuming uniform suction from the UTC perforations, according to Kutscher (1994), considering the mass flow entering the exposed UTC area and the PV covered area for the energy balance.

Yang et al (2014) studied experimentally a BIPV/T prototype, previously studied outdoors by Candanedo et al (2011), in the Solar Simulator facility of Concordia University. The single-inlet prototype was a scaled version of the system installed in EcoTerra (Chen, 2010). The flow rate inside the air channel was controlled by an air collection unit, while the Reynolds number was kept below 10,000 in order to keep frictional losses low. Yang developed Nusselt correlations for the laminar and the turbulent region for both the PV and the insulation layer of the collector, which were used to model an improved design with two inlets, intended for inclined roof applications. In order to further enhance the thermal performance of the system, a vertical glazed solar collector part added to the BIPV/T system was also modelled. It was found that the thermal efficiency of the two-inlet system was 5% higher than that of the single-inlet prototype. Furthermore, there was a 1.5^{o}C decrease in the peak PV temperature, as well as a marginal increase in the electrical efficiency of the system. It was expected that for larger roof installations of 5-6 m the temperature decrease would be from 5-10^{o}C, depending on the flow rate and the wind conditions. Such a reduction in peak PV temperature would also mean slower PV degradation.

Mizraei et al (2014) investigated experimentally the role of cavity flow on the performance of BIPV/T placed on inclined roofs. The experimental configurations included a flat and a stepped arrangement, which was essentially a multiple-inlet formation. The cavity was naturally ventilated and no mechanical air collector potential was investigated; however, it was found that the PV temperatures were significantly lower for the stepped configuration cases, as opposed to the flat roof.

All aforementioned studies assumed uniform air intake from all system openings, while neglecting the wind effects on the flow distributions of the system. However, the flow distributions of such a system, depending on the system's geometric features and wind conditions, may be far from uniform. It is therefore important to model these flows, since they define the systems performance, in terms of internal convection. This study focuses on the development of a multiple-inlet BIPV/T model, which addresses both the inlet flow distributions and the energy performance of the system. The potential performance of a multiple-inlet system, based on a large installation case study, is investigated with the aim to improve the PV temperatures, as well as the electrical and thermal gains, as opposed to a typical single inlet system.

MULTIPLE-INLET BIPV/T MODELLING

The modelling of a multiple-inlet system includes two parts: the flow modelling aspect and the energy balance.

Contrary to the typical systems consisting of a continuous air channel and, therefore, a single flow rate, multiple-inlet systems have by definition different flow conditions in every separate channel. These flow conditions are based on the inlet flows and define two important parameters for the energy balance modelling; namely the flow rate of each channel and the boundary temperature of air entering each channel. The amount of air entering each opening of a multiple-inlet system depends on the geometry of the opening and of the flow channel, the total mass flow of the air collector and the effect of wind. Both flow and energy modelling are based on finite control volume techniques, with every PV module and its corresponding cavity/channel forming a control volume.

Flow modelling

The inlet and the channel flows of a multiple-inlet BIPV/T system form a complex flow network with interconnected flow paths that cannot be directly evaluated. A useful representation of flow networks, especially when dealing with complex flows, is the electrical analogy (Aynsley, 1997). Pressure drop is related through a proportionality constant, or flow resistance, to the flow in an equivalent manner as voltage is linked to electrical current and the rules of addition of resistances in series or in parallel are applied. The main pressure drop-flow correlations used are the orifice equation and the Darcy-Weisbach equation for frictional pressure drop:

- The orifice equation:

$$\Delta P = \frac{1}{2} \cdot K \cdot \rho \cdot Q^2 / A^2 \quad (1)$$

Q is the flow rate (m^3/s), ΔP the pressure drop across the orifice (Pa), A the orifice area (m^2), ρ the density of the fluid (kg/m^3), C_D the discharge coefficient for the orifice (dimensionless) and K the loss coefficient for flow through an orifice (dimensionless)

- The Darcy-Weisbach equation:

$$\Delta P = f \cdot \frac{L}{D_h} \cdot \frac{\rho \cdot V^2}{2} \quad (2)$$

ΔP is the pressure drop across the air collector (Pa), L is the length of the air collector (m), D_h is the hydraulic diameter of the air channel (m), ρ is the air density (kg/m^3) and V is the average air velocity inside the air channel (m/s). There are several methods for solving complex flow networks the branches of which form closed loops, such as the Hardy Cross method, which can calculate the flow through an infinite number of loops and nodes making use of the first two laws of Kirchoff:

- The quantity of air entering a junction must be equal to the quantity of air exiting the junction (mass continuity)
- The summation of pressure drops around any closed path is zero (potential/energy continuity)

These methods have been mainly used for the investigation of wind-driven flows and pressure distributions in buildings and compartmentalized double screen facades (Lou et al, 2012; Aynsley, 1997; Dymond & Kutscher (1997)) used pipe networking methods to develop a simple computer algorithm for the calculation of the flow distributions in transpired solar collectors, in an effort to create a design guideline to counter the poor flow distribution occurring in large building installations. The absorber was modelled with a three-dimensional set of fictitious pipes and using relations for pressure drop across the plenum, within the air collector, due to buoyancy and due to flow acceleration. A major assumption of the model was that wind effects were considered insignificant and were not modelled based on the fact that if the pressure difference across the absorber is more than 25 Pa, wind does not affect the flow across the absorber.

The electrical analogy is employed in this study for the modelling of the complex flow network that is formed within a multiple-inlet BIPV/T system. A schematic of this general flow network is shown in Figure 2:

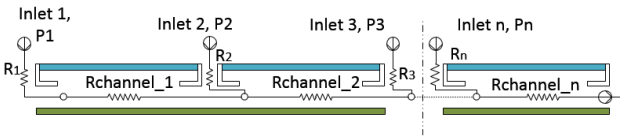

Figure 2: Electrical resistance analogy for flow modelling of a BIPV/T system with multiple openings.

The wind effects, represented as equivalent exterior pressure sources, and interior nodes of two consecutive inlets form a closed loop, similar to the pipe networks adopted by Dymond and Kutscher (1996). The main principles upon which the flow modelling is based are mass continuity (3) and conservation of mechanical energy (4):

$$\sum_{i=1}^{n} Q_{opening(i)} = Q_{tot} \quad (3)$$

$Q_{opening(i)}$ is the flow through the i-th opening of the system (m^3/s) and Q_{tot} is the total air collection rate from the system's fan (m^3/s).

Conservation of mechanical energy is applied to each of the closed loops formed in the flow network in the form

of pressure drop. The sum of pressure drops in a closed loop should be equal to zero, as expressed by the following relationship:

$$\Delta P_{opening\,(i)} + \Delta P_{\text{channel}(i)} - \Delta P_{opening\,(i+1)} + P_{(i+1)} - P_{(i)} = 0 \quad (4)$$

$\Delta P_{opening(i)}$ is the pressure drop from flow across the i-th inlet (flow through an orifice) (Pa), $\Delta P_{channel(i)}$ is the frictional pressure drop from flow within the i-th air channel, as well as from flow through the back frame of the PV panels (Pa) and $P_{(i)}$ is the pressure exterior to the i-th inlet, defined by the local wind effects (Pa).

It is assumed that the system employs a variable speed fan which at all times provides a constant air mass outflow.

Pressure drops

There are two types of pressure drop in a multiple-inlet system: from flow across the inlets and from flow within the air channel. The system's inlets are less than 2% of the BIPV/T area, therefore, according to Lo et al (2012), pressure-driven flow may be assumed and the orifice equation employed to describe the pressure drop from flow across the inlets. The pressure drop from flow within the air channel is a combination of frictional losses, described by the Darcy-Weisbach equation, as well as pressure drop from flow across the back part of the air channel, due to the resistance caused by the frame of the PV panels, in case of a framed configuration. Since the latter creates a sharp entrance, the orifice equation is also employed.

The friction factor *f*, used in the Darcy-Weisbach equation, was implemented through empirical correlations for the modelling process:

For laminar flow (Re<2300):

$$f = 64 / \mathrm{Re} \quad (5)$$

For the turbulent regime, several empirical relationships have been suggested. The one used in this study is the one also used by Ghani et al (2012), as it also has good agreement of results with equation (5) for the laminar region:

$$f = (0.79 \cdot \ln(\mathrm{Re}) - 1.64)^{-2} \quad (6)$$

The local pressure exterior to the inlets of the system is a result of local wind effects. The wind-induced pressure on the BIPV/T area was measured at the Boundary Layer Wind Tunnel of Concordia University for a test model of an office building, for various wind directions, dictated by the local prevailing wind conditions. The measurement results were recorded in terms of pressure coefficients, dimensionless ratios of local wind induced pressure over the dynamic wind pressure, which is independent of the wind velocity and depends only on the wind direction and the local geometric features.

$$C_P = \frac{P_s}{\frac{1}{2} \cdot \rho \cdot V_{loc}^2} \quad (7)$$

P_s is the surface pressure (Pa), C_p is the pressure coefficient for a given wind direction (dimensionless), ρ is the air density (kg/m^3) and V_{loc} is the velocity of wind at the height of measurement (m/s). The acquired pressure coefficients were used as input in the mechanical energy conservation equations of the flow loops described above, in a similar way as Lo et al (2012) used wind tunnel acquired pressures as boundary conditions for CFD simulations.

Electrical analogy

The complex flow network of a multiple-inlet BIPV/T is modelled in this study employing the electrical circuit analogy. The pressure drop is thus correlated to the flow with a resistance:

$$\Delta P = Q \cdot R \quad (8)$$

The resistances are derived from the linearization of equations (1) and (2):

- Inlet Resistance

$$R_{inlet} = \left(\frac{K_{inlet}}{A_{inlet}^{\,2}}\right) \cdot \frac{Q_{inlet}}{2} \cdot \rho \quad (9)$$

- Channel resistance

$$R_{channel} = \left(\mathrm{f} \cdot \frac{L}{D_h} + K_{b.\,frame}\right) \cdot \frac{Q_{channel}}{2 \cdot A_{b.\,frame}^{\,2}} \cdot \rho \quad (10)$$

$R_{opening}$ and $R_{channel}$ are the resistances of the inlet and the air channel respectively (kg/(m^4.s)), K_{inlet} and $K_{b.frame}$ are the K factors of the inlet and the back part of the PV frame, A_{inlet}, $A_{channel}$ are the cross sectional area of the inlet and the air channel respectively (m^2), L is the length of the air channel (m), D_h is the hydraulic diameter of the air channel (m), f is the friction factor, Q_{inlet} and $Q_{channel}$ are the volumetric flow rate through the inlet and the air channel respectively and ρ is the air density (kg/m^3).

The pressure drops due to flow across an inlet and through an air channel can now be written as follows:

- Inlet pressure drop:

$$\Delta P_{inlet} = Q_{inlet} \cdot R_{inlet} \quad (11)$$

- Channel pressure drop:

$$\Delta P_{channel} = Q_{channel} \cdot R_{channel} \quad (12)$$

All the above equations can be rewritten in a matrix form as follows:

$$[R] \cdot \{Q\} = [P] \quad (13)$$

[R] is the matrix containing the resistances for the mechanical energy conservation equations the continuity of mass equation, {Q} is the vector with the unknown inlet flows and [P] is the vector containing the constants of the external pressure differences and the total air collector volumetric flow.

The relationship between pressure difference and flow is non-linear. Inlet and channel flows are used within the resistances in order to produce a system of equations with a linear form for the matrix solution.

Wind effects and energy balance

Wind, depending on the angle of attack and its velocity, may cause varying pressure distributions over the BIPV/T area. These pressure variations are expected to affect the multiple-inlet system flow distributions. The possible flow paths for the inlet and the channel flows are shown in Figure 3:

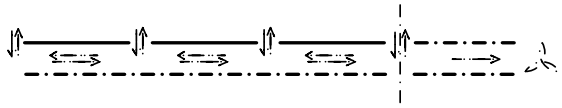

Figure 3: Possible flow paths for the inlets and channels of the multiple-inlet system.

The channel flows will in turn affect the internal convection part of the energy balance, while the direction of the flows of the inlets and the channels will define the temperature of air entering each channel.

Multiple-inlet BIPV/T energy balance

The energy balance of a multiple-inlet BIPV/T is modelled using the finite control volume method, with each of the separate channels (and PV modules) of the system comprising a control volume (CV). The main difference from the known BIPV/T energy balance is that each CV has a different flow rate and air temperature boundary conditions. The energy balance concept for a multiple inlet system is shown in Figure 4:

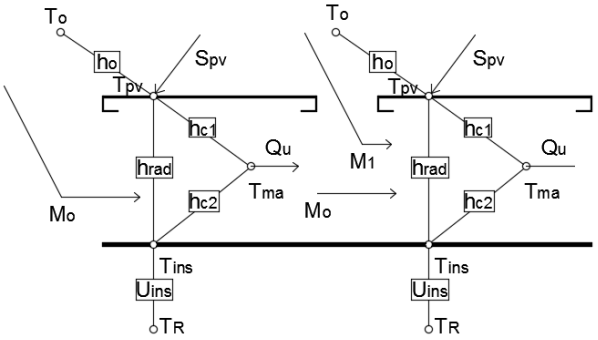

Figure 4: Multiple-inlet BIPV/T energy balance.

T_o is the external temperature (^oC), h_o is the exterior film coefficient ($W/m^2.^oC$), T_{PV}, T_{ma}, T_{ins} and T_R are the temperatures of the PV the air inside the air channel, the surface of the insulation and the adjacent room respectively, h_{c1}, h_{c2} are the convective heat transfer coefficients from the PV and the insulation surface to the flowing air respectively ($W/m^2.^oC$), h_{rad} is the radiative heat transfer between the PV and the insulation surfaces ($W/m^2.^oC$), S_{PV} is the net heat absorbed by the PV layer (total absorbed-electric produced) (W/m^2), ρ is the density of air (assumed constant), ($1.2kg/m^3$), C_p is the specific heat capacity of air, assumed constant (1000 $J/kg.^oC$) and M is the mass flow rate inside the collector, assumed constant (kg/s).

Figures 5 demonstrates the various cases of flow conditions for the inlets and the channels, as well as the resulting boundary conditions for the air temperature entering each control volume. Q_{inlet_n} is the flow through the n-th inlet (m^3/s), Q_{n-1} is the flow from the (n-1)-th CV (m^3/s), Q_n is the flow of the n-th CV (under investigation) (m^3/s), T_{air} is the ambient air temperature (^oC), T_{n-1} is the temperature of air from the (n-1)-th channel (^oC) and T_i, T_o are the air temperature at the entrance and at the exit of the air channel respectively (^oC).

For each channel/CV, the subscript "i" denotes the end of the n-th CV closer to the n-th inlet, while the subscript o refers to the end closer to the system's outlet.

Modelling assumptions

The secondary loss factors (K) used in the flow distribution model were assumed from the literature (ASHRAE) on duct design. Furthermore, the Nusselt number correlation used in this study were those developed by Yang (2014), who studied a similar system with 2 inlets and performed a numerical study on a four-inlet system.

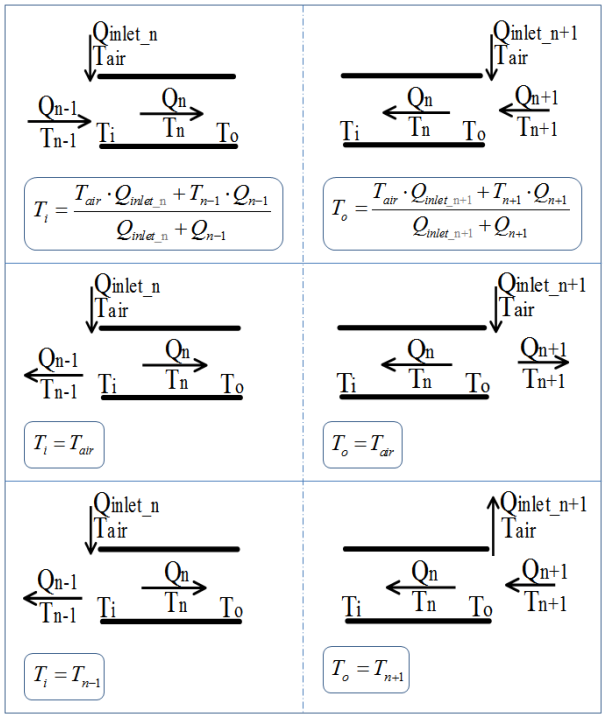

Figure 5: The six possible channel flows and channel air temperature inlet boundary conditions.

The wind effects investigated in this study concerned with the effect of wind induced pressure distributions on the inlet flow distribution. An average relationship between local wind velocity and external convection was used, similar to those developed by Liu & Harris (2007):

$$h_{wind} = 6 \cdot V_{loc} + 4 \quad (14)$$

For simplicity, only one wind reference speed is considered and not the actual velocity distributions over the BIPV/T area. This, according to Vasan and Stathopoulos (2014) may lead to overestimation of the heat exchange efficiency and underestimation of the wind-induced losses.

WIND TUNNEL MEASUREMENTS

Figure 6 shows the wind tunnel model and the building orientation, with its outline placed on the wind rose for Montreal, as well as the wind directions tested.

The available 80 m x 10 m retrofit area of the actual building was assumed to be covered by 2 m x 1 m PV modules, thus forming 40 PV strings of 10 modules each. That was represented in the wind tunnel model by a 203 mm x 27.5 mm Plexiglas face equipped with 28 pressure taps as shown in Figure 7.

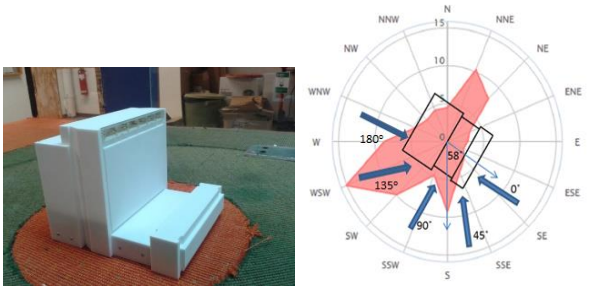

Figure 6: 1:400 scaled model of the building (left) and building orientation, wind diagram for Montreal and wind directions tested (right).

Figure 7: BIPV/T façade for the wind tunnel model, equipped with pressure taps.

It is difficult to generalize wind measurements on buildings due to the high variation of building shapes, as well as the local surrounding that highly influence the wind patterns. For this reason, a typical open field exposure was chosen, with a flow exponent of α=0.13, as a first step to assess the expected effect of wind on the multiple-inlet BIPV/T flow distributions. The open field was chosen, although the building is located in an urban area, since it was expected to produce more severe wind conditions.

Figure 8 demonstrates the pressure coefficient contours for five angles of oncoming wind over the BIPV/T area, as acquired through the wind tunnel testing:

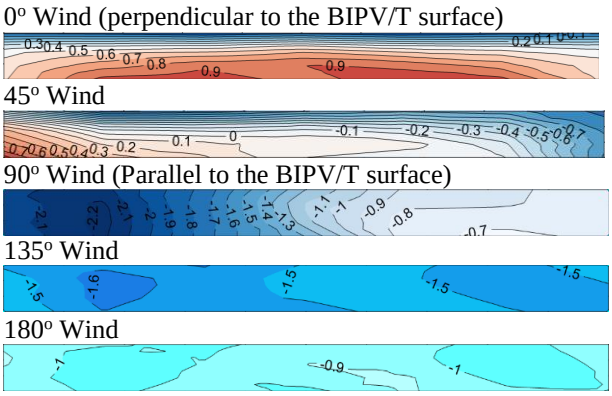

Figure 8: Pressure coefficient distributions on BIPV/T area. From top to bottom: 0º, 45º, 90º, 135º and 180º angles of incidence of wind.

The first, and primarily the second case, (45º wind), created the highest pressure coefficient distributions in the vertical sense. For a PV string, placed along the installation height, this would mean highly varying

pressure values at each inlet of the system which could lead to outflow at the locations under suction for an improperly designed system.

The rest of the tested wind directions resulted in either uniform pressure coefficient distributions over the BIPV/T area (135° and 180°) or vertical regions of the same pressure conditions (90°) which would have small effect on the flow distributions.

SIMULATIONS

The models developed in the previous chapter were used for the numerical investigation of the performance of two single and two multiple-inlet BIPV/T systems considered for an office building application. The goal of these simulations was twofold:

1. Investigate the flow distributions of the multiple-inlet systems in relation to the system's geometry, total flow rate and wind effects.
2. Investigate the performance of a multiple-inlet system against a single-inlet, for typical Montreal weather conditions. The systems were compared in terms of electrical and combined electrical-thermal efficiency, as well as PV temperature uniformity, which is a major factor of consideration for the durability of large PV installations.

Conditions considered

The simulations were carried out for a cold winter and a hot summer day. The temperature was defined in a sinusoidal form with an average value of -15°C and 20°C for the cold and the hot day respectively, with a ±5°C swing and a peak at 3 pm. The solar irradiation was calculated assuming clear days for a surface azimuth of -58°, according to the actual building orientation. For the wind effects, three wind directions were considered: that of 45°, as the case with the highest variations and those of 90° and 135° as the prevailing wind directions for the particular location. Wind velocities up to 2 m/s were used, since higher wind speeds resulted in high external convection that dominated the energy balance, thus producing small differences in the energy performance and PV temperatures of the assumed systems.

BIPV/T systems considered

For the simulations, two single inlet systems were considered as a reference technology and two multiple-inlet systems. The PV modules were assumed to have a nominal efficiency of 15% and therefore an output of 300 W. Thus the 40 PV strings formed a 120 kW system. The two single and the two multiple-inlet systems were identical in terms of PV module and opening configurations but varied in the channel gap size. The two channel gaps for each type of system were 0.10 m and 0.15m, in order to account for the effect of the channel gap size to the flow and internal convection. Furthermore, two total mass outflows from the air collector were considered, namely 400 kg/h and 800 kg/h (resulting in maximum channel air velocities of 0.5 m/s and 1 m/s respectively) to account for the effect of total air flow on the flow distributions and the energy balance of each channel. All systems were based on framed PV modules 2 m wide and 1 m long along the flow path of air inside the air channel, thus creating 10 m long and 2 m wide PV strings. The openings of the multiple-inlet systems, given in the form of inlet porosities (inlet area over PV module area) are shown in Table 1.

Table 1: Inlet porosities for the multiple-inlet systems.

Inlet	Porosity (%)
1	10
2	1
3	0.5
4	0.5
5	0.3
6	0.2
7	0.1
8	0.01
9	0.01
10	0.01

These porosities were a result of a heuristic design of the system's inlets, which was carried out in two steps: first, the required flows in order to have uniform PV temperatures were evaluated through a trial and error procedure using the energy balance model. This was carried out for no wind conditions, where the highest PV temperatures were expected. Secondly, having acquired the required flows through each inlet, the flow model was used in order to size the inlets accordingly.

RESULTS AND DISCUSSION

This section presents the main findings of the simulations concerning the flow distribution of the multiple-inlet systems in respect to the parameters that affect it, as well as its performance in terms of expected electrical and thermal efficiency and PV temperatures, as compared to the single inlet systems.

Flow distribution

Figure 9 demonstrates the inlet flows of the two multiple-inlet systems, as calculated for the case of 2m/s wind approaching at a 45° angle, as well as for the case of uniform exterior pressure (no wind) normalized by a total flow rate of 400 kg/h. The vertical axis corresponds to the inlet openings 1 (bottom) through 10 (top) of the

system, while the horizontal axis shows the calculated inlet flows, normalized by the total air mass outflow of the air collector. The error bars indicate the variations of the inlet flows for the 40 PV strings of the BIPV/T system from the average flow of the corresponding inlet, due to the pressure distributions induced by the 45° degree over the BIPV/T area.

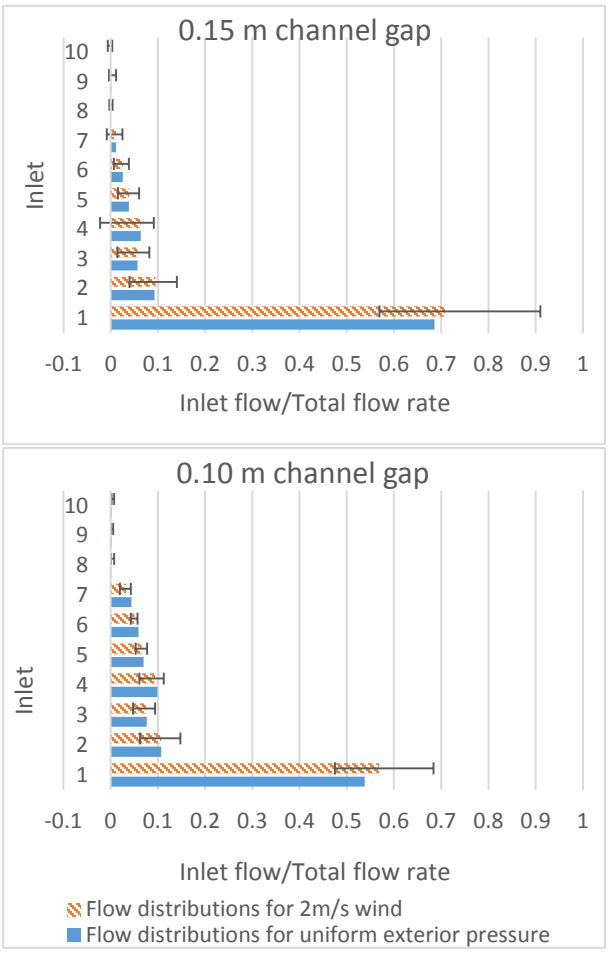

Figure 9: Normalized flow distributions of multiple-inlet systems with a 0.15 m and 0.10 m channel gap, for 2 m/s wind at 45° angle of incidence and 400 kg/h total flow rate.

Effect of channel gap size

The reduced gap size increases the resistance to the flow both in terms of increased friction, as well as reduced flow area, since the opening created by the back part of the PV frame and the back wall becomes smaller. This results in reduced inlet flows for the inlets that are located the farthest from the outlet for the system with the reduced gap size (0.10 m). Furthermore, the increased resistance decreases the effect of wind on the flow distributions, as it is clear from the smallest inlet flow variations for the system with smaller gap (0.10 m).

Effect of wind and total mass flow rate

The simulations were carried out for two total mass flow rates, 400 kg/h and 800 kg/h. It was found that by changing the total mass flow rate, the ratios of the inlet flows tot the total air collection rate remained the same. Furthermore, a higher air collection rate minimized the wind effect on the flow distribution to negligible variations from the designed inflows. A total air collection rate for such a system results in an air velocity within the air channel of approximately 1 m/s, which is typical for BIPV/T systems.

Concerning the effect of wind, the case of 2 m/s wind at 45° resulted in the highest variation of the inlet flows, as opposed to the designed flow distributions, for an air collection rate of 400 kg/h. the rest of the assumed wind directions produced much smaller variations, mainly due to the fact that they produced very uniform pressure coefficient distributions over the BIPV/T area. With a higher air collection rate of 800 kg/h, these variations became even smaller. Wind velocities of 3 m/s and higher were found to produce more considerable variations, they were however not studied further, since they resulted in similar system performances, as the dominating external convection keeps the PV temperatures low and rather uniform in all cases.

PV temperatures

Figure 10 demonstrates the PV temperatures that correspond to the inlet flows caused by a 2 m/s wind approaching at 45°, i.e. cases presented in Figure 9. The vertical axis of Figure 10 indicates the 10 PV modules of the PV string and the horizontal axis the PV temperatures as calculated due to the inlet flow distributions as previously. The error bars indicate the variations of the PV temperatures for the 40 PV strings of the BIPV/T system from the average flow of the corresponding inlet, due to the inlet flow distributions induced by the 45° degree wind over the BIPV/T area. The plots are for summer conditions, when the highest PV temperatures are expected, for the two channel gap sizes (0.10 m and 0.15 m) and the two total air collector flow rates (400 kg/h and 800 kg/h) .

Results showed the following

- Even the high variations in inlet flows (Figure 9) result in insignificant temperature variations, from those that would be expected according to the designed flows (±3°C for the system with 0.15 m channel gap and total mass air flow rate of 400 kg/h).

- The system with 0.10 m channel gap has smaller temperature variations which correspond to the smaller inlet flow variations.
- The variations are almost eliminated when the total air collection rate is doubled. The 800 kg/h air collection rate corresponds to a channel air velocity of approximately 1 m/s which is typical for BIPV/T systems.
- The velocity of wind is much more crucial than the actual direction on the PV temperatures, concerning the wind effect on the internal convection.

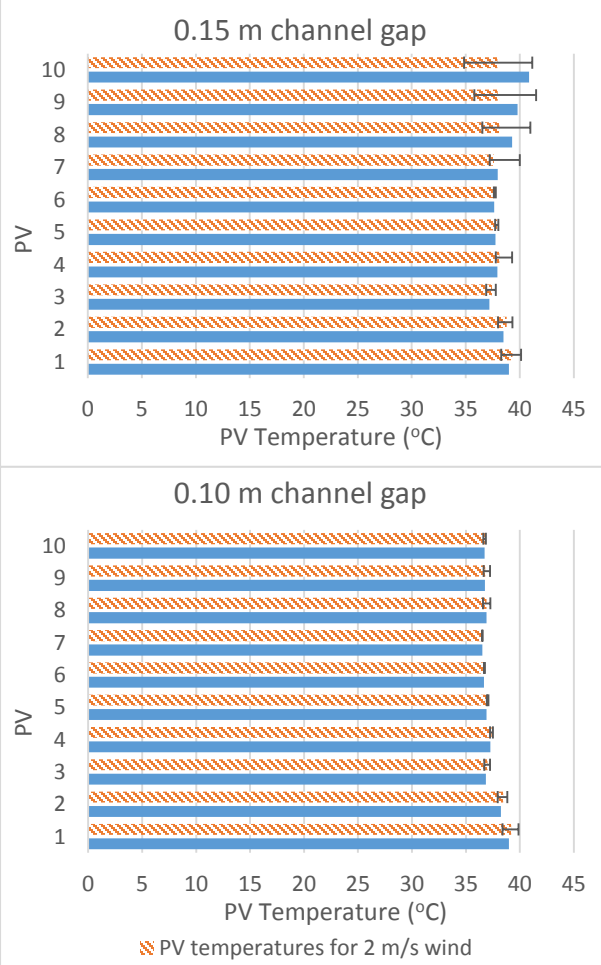

Figure 10: PV temperature distributions of multiple-inlet systems with a 0.15 m and 0.10 m channel gap, for 2 m/s wind at 45° angle of incidence and 400 kg/h total mass flow rate.

The temperature variations were minimal for the other two wind directions. Higher wind velocities were not examined since although with increasing wind velocity the inlet flow variations increase, so does the wind driven convection, which dominates the energy balance resulting in low and uniform PV temperatures. Winter PV temperatures follow a very similar pattern but with much lower PV temperatures.

Figure 11 presents a comparison on the uniformity of the modules' temperatures of an average PV string for 400 kg/h, for summer conditions and three wind velocities for the single and multiple-inlet system with 0.15 m channel gap. Results showed that an increase of the total air mass flow of the air collector yields lower PV temperatures, the differences being more prominent at conditions with no wind. However, with increasing wind velocity, external convection dominates and the differences are lower. This also results in lower PV temperature variations along the same string. In all cases, the multiple-inlet systems had uniform PV temperature distributions, with small temperature differences between panels and with the lowest overall PV temperatures. The same profile of PV temperatures was evident for the winter conditions, the higher air collector flow rate, as well as the 0.10 m channel gap systems. Even at a lower total mass flow rate of the air collector, the multiple-inlet system maintains low and uniform PV temperatures along the PV string.

Electrical and thermal efficiency

The efficiencies of the BIPV/T systems considered for the simulations were calculated as follows:

- Daily electrical efficiency: Total electrical energy produced over the total daily solar irradiation incident on the BIPV/T surface.
- Daily combined efficiency: The sum of the total daily electrical energy produced and thermal energy extracted and transferred to the air flowing inside the air channel over the total daily solar irradiation incident on the BIPV/T surface.

The results showed that the multiple-inlet systems could have up to 1% higher electrical efficiency (which for a 120kW system would translate to 7% higher production) and from 14% to 25% higher thermal efficiency depending on the conditions.

The differences in the electrical efficiency of the single and the multiple-inlet systems became smaller with increasing wind velocity, due to the lower PV temperatures. In accordance with previous studies, increasing total air collection flow rate resulted in higher thermal efficiencies. This is also the case for each system configuration, with the gap size of the air channel reduced, which results to higher air velocity inside the air channel and higher internal convection.

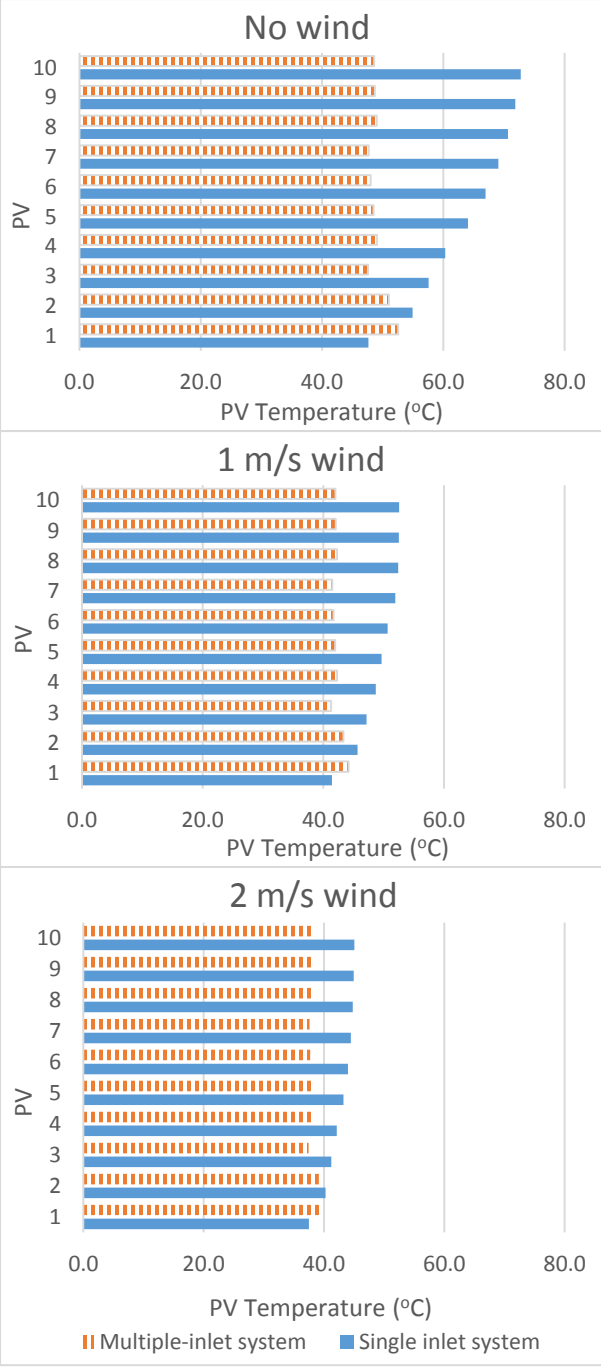

Figure 11: Comparison of PV temperatures for single and multiple-inlet systems for no wind, 1 m/s and 2 m/s wind and 400 kg/h total mass flow rate.

CONCLUSION

Multiple-inlet BIPV/T systems are expected to operate at lower PV temperatures and have higher electrical and thermal efficiency, as compared to a single inlet system. This study introduced a methodology for the modelling of such systems. The methodology includes a flow distribution model, which incorporates wind effects in the form of exterior pressures, and a simple energy balance model that accounts for the various cases of flow conditions for the inlets and the air channels of the system.

The proposed approach was applied to the numerical investigation of variations of multiple-inlet BIPV/T systems considered for a potential retrofit project of an office building. Results were compared with single inlet system designs for the same environmental conditions. The comparison showed the following:

- A multiple-inlet system, the inlet flows of which have been designed for the highest heat extraction from all the PV modules of the system for no wind conditions, outperforms a single inlet system in terms of PV temperature uniformity, electrical and thermal efficiency, under all types of weather conditions assumed in this study.
- For the single inlet system, the temperature difference between the warmest and the coolest PV panels may vary from 8 to 26°C, depending on the conditions, while the temperature of the warmest panel may exceed 70°C. For the multiple-inlet system, the corresponding temperature difference is 3 to 7°C, and the maximum PV temperature is 53°C. The lower operating temperatures of an optimized system may be of significant importance for the durability and maintenance of large PV installations.
- An increase of up to 1% in electrical efficiency was observed for the multiple-inlet system. For a 120 kW system, this translates in 7% higher electrical production. Furthermore, there was a 14% to 25% increase in the thermal efficiency, in comparison to the single inlet system, depending on the weather conditions.

The effect of wind direction on the flow distributions and as a result to the internal convection part of the energy balance was found to be insignificant for wind velocities up to 2 m/s, regardless of the wind direction. Higher wind velocities would be expected to cause more considerable differences; however, with external convection dominating, the performance of all systems investigated would be similarly affected, in that the PV temperatures would be low and uniform, while the thermal gains would be minimal.

ACKNOWLEDGMENTS

The authors acknowledge the support of the Natural Sciences and Engineering Research Council of Canada (NSERC) through a NSERC/Hydro Quebec Industrial Chair.

REFERENCES

ASHRAE, 2009, -ASHRAE Handbook of Fundamentals, American Society of Heating, Refrigerating and Air-Conditioning Engineers, Atlanta, GA, USA

Athienitis, A.K., Bambara, J., O'Neill, B., Faille, J. (2010). A prototype photovoltaic/thermal system integrated with transpired collector. *Solar Energy* 85, 139-153

Aynsley, R.M. (1997). A resistance approach to analysis of natural ventilation airflow networks. *Journal of Wind Engineering and Industrial Aerodynamics* 67&68, 711-719

Bambara, J., Athienitis, A.K., Karava, P. (2012) Performance Evaluation of a Building-Integrated Photovoltaic/Thermal System. International High Performance Buildings Conference, 2012, Purdue

Candanedo, L.M., Athienitis, A.K., Candanedo, J.A., O'Brien, W., Chen, Y. (2010) Transient and steady state models for open-loop air based BIPV/T systems, American Society of Heating, Refrigerating and Air-Conditioning Engineers. Transactions 2010, Vol.116, Part 1, 600-612

Chen, Y., Athienitis, A.K., Galal, K. (2010). Modeling, design and thermal performance of a BIPV/T system thermally coupled with a ventilated concrete slab in a low energy solar house: Part 1, BIPV/T system and house energy concept. *Solar Energy* 84, 1892-1907

Dymond, C., Kutscher, C. (1997). Development of a flow distribution and design model for transpired solar collectors. Solar Energy 60, 291-300

Florschuetz, L.W. (1979). Extension of the Hottel-Whilier model to the analysis of combined photovoltaic/thermal flat plate collectors. *Solar Energy* 22, 361-366

Ghani, F., Duke, M., Carson, J.K. (2012). Effect of flow distribution on the photovoltaic performance of a building integrated photovoltaic/thermal (BIPV/T) collector. *Solar Energy* 86, 1518-1530

Hegazy, A.A., (1999). Comparative study of the performances of four photovoltaic/thermal solar air collectors. *Energy Conversion & Management* 41, 861-881

Kutscher, C.F. (1994). Heat exchange effectiveness and pressure drop for air flow through perforated plates with and without crosswind. *Journal of Heat Transfer* 116, 391-399

Lo, L.J., Banks, D., Novoselac, A. (2012). Combined wind tunnel and CFD analysis for indoor airflow prediction of wind-driven cross ventilation. *Building and Environment* 60, 12-23

Lou, W., Huang, M., Zhang, M., Lin, N. (2012). Experimental and zonal modeling for wind pressures on double-skin facades of a tall building. *Energy and Buildings* 54, 179-191

Mizraei, P.A., Paterna, E., Carmeliet, J. (2014). Investigation of the role of cavity airflow on the performance of building-integrated photovoltaic panels. *Solar Energy* 107, 510-522

Tonui, J.K. & Tripanagnostopoulos, Y. (2006). Air-cooled PV/T solar collectors with low cost performance improvements. *Solar Energy* 81, 498-511

Vasan, N., Stathopoulos, T. (2014). Experimental study of wind effects on unglazed transpired collectors. *Solar Energy* 101, 138-149

Yang, R.J. (2014). Overcoming technical barriers and risks in the application of building integrated photovoltaics (BIPV): hardware and software strategies. *Automation in Construction* 51, 92-102

Yang, T., Athienitis, A.K. (2014). A study of design options for a building integrated photovoltaic/thermal (BIPV/T) system with glazed air collector and multiple inlets. *Solar Energy* 104, 82-92